激光与光电子学进展 先进成像

微观探索的新光芒:便携式光声显微成像技术(特邀)

孙明丽,李驰野,陈睿黾,施钧辉*
之江实验室类人感知研究中心,浙江 杭州 311121

摘要 光声成像(PAI)是一种结合了光学成像高对比度和超声成像深穿透性的生物医学成像模态,近年来得到了迅速发展。其中,光声显微成像(PAM)作为光声成像的重要实现方式之一,可以在毫米级的成像深度上实现微米级甚至百纳米级的分辨率,能够实现对生物组织结构、功能和分子的高分辨率成像,已在临床诊断、皮肤病检测和眼科等领域得到广泛应用。首先对PAM的工作原理和实现方式等进行基本介绍,之后围绕便携式PAM技术,从手持与半手持式、脑部可穿戴式及集成多模态3方面对其研究进展进行综述,随后探讨便携式PAM技术面临的挑战,最后进行总结与展望。

关键词 生物医学成像; 光声成像; 光声显微成像; 便携式光声显微成像
中图分类号 R318 **文献标志码** A **DOI**: 10.3788/LOP232623

New Light in Microscopic Exploration: Portable Photoacoustic Microscopy (Invited)

Sun Mingli, Li Chiye, Chen Ruimin, Shi Junhui*
Research Center for Humanoid Sensing, Zhejiang Lab, Hangzhou 311121, *Zhejiang, China*

Abstract Photoacoustic imaging (PAI), a biomedical imaging mode that combines the high contrast of optical imaging with the deep penetration of ultrasonic imaging, has developed rapidly in recent years. Among them, photoacoustic microscopy (PAM), as one of the important implementation methods of photoacoustic imaging, can achieve micron-level or even hundreds of nanometer-level resolution on the millimeter imaging depth, and can achieve high-resolution imaging of biological tissue structure, function, and molecules, and has been widely used in clinical diagnosis, skin disease detection, ophthalmology, and other fields. In this paper, the working principle and implementation of PAM are first introduced, and then the research progress of portable PAM technology is reviewed from the handheld and semi-handheld, brain wearable, and integrated multi-mode. Then, the challenges faced by the portable PAM technology are discussed, and finally the prospects are summarized.

Key words biomedical imaging; photoacoustic imaging; photoacoustic microscopy; portable photoacoustic microscopy

1 引 言

在生物医学领域,诸如眼科、皮肤科、内窥等方面,需要对微血管网络进行成像,传统的X射线断层成像(X-CT)有电离辐射并且需要用到造影剂;磁共振成像(MRI)费用昂贵,且空间分辨率也只有1 mm级别;光学相干层析成像(OCT)无辐射、成像速度快、分辨率高,但是由于生物组织对光的强烈散射,光难以在组织内聚焦,无法观测较厚的生物组织;近年来,光声成像(PAI)因无损伤性、高分辨率、大穿透深度等特点,成为生物医学影像领域的重要研究内容[1-5]。传统的光学成像由于组织内光学散射远高于声散射导致深度分辨率严重下降,而超声成像可以实现对深层生物组织的成像,但其在分辨率和对比度方面不足。PAI融合了二者的优点,不仅能够直接成像生物组织的光吸收分布,还有效结合了光学成像的高对比度和高分辨率、超声成像的大穿透深度的优势,无需外源性标记就能实现对生物组织的更深层成像。

光声显微成像(PAM)作为PAI的重要分支,成像深度可达数毫米,空间分辨率可达几微米甚至百纳米[6-12]。与传统的光学显微镜(如共聚焦、双光子显微镜)或光学相干层析成像相比,PAM有独特的优势:利用超声探测,可以克服光学散射极限,获取更深的组织信息;能以高灵敏度获取微血管的结构和功能信息;无

收稿日期: 2023-12-05; **修回日期**: 2024-01-09; **录用日期**: 2024-01-15; **网络首发日期**: 2024-01-26
基金项目: 之江实验室青年基金(K2023MG0AA12)
通信作者: *junhuishi@outlook.com

须依靠光学切片即可获得三维体图像。它可以利用内源性或外源性造影剂进行结构、功能和分子成像，目前已广泛应用于许多领域，包括生物组织学[13-15]、肿瘤学[16-20]、神经科学[21-23]、眼科学[24-26]及皮肤学[27-28]等。近些年，人们致力于从各个方面提高PAM的成像性能与实用价值，为了适应不同的应用场景，体积小、易于携带、性能佳的便携式PAM系统是发展的必然趋势。为了促进读者对该领域的了解，本文聚焦于便携式PAM技术，首先对PAM的工作原理、实现方式等进行介绍，之后从手持与半手持式、脑部可穿戴式及集成多模态3方面对便携式PAM的研究进展进行综述，最后探讨便携式PAM技术面临的挑战，并展望未来技术的发展方向。

2 光声显微成像技术

光声成像的物理基础源于1880年Bell[29]发现的光声效应。它的基本原理[30]如图1所示。当生物组织受到短脉冲激光或强度调制激光照射时，组织吸收的能量不能在短时间内释放，导致瞬间温度变化，随后热弹性机制引起体积的涨缩，使周围的介质发生胀缩而激发超声波。通过探测超声信号，重构出反映生物组织光吸收分布的图像，从而反映生理学特征[31-32]。光声成像通过探测时间序列上的超声而具备层析能力，可以利用血液在可见光波段的吸收要远远高于其他组织（除黑色素之外）的特点实现内源性无标记成像。

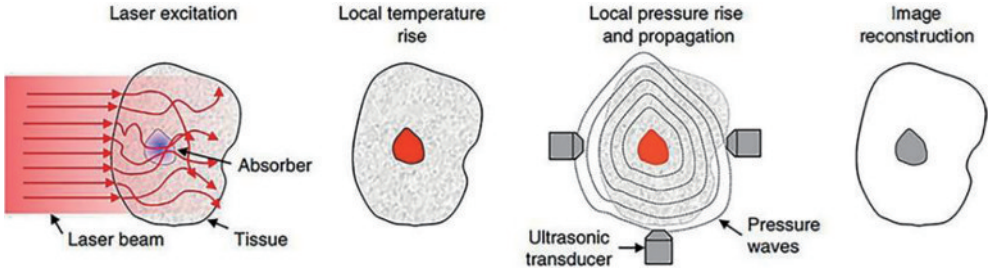

图1 光声成像原理[30]

Fig. 1 Schematic of photoacoustic imaging[30]

光声显微成像具有较高的空间分辨率，通常采用单阵元超声探头进行逐点扫描探测。每个激光脉冲获取光声A-line深度信号，该信号携带时间飞行信息，能够用于分辨物体深度信息，一维线扫描产生光声B-scan图像，二维栅格扫描获得物体的三维图像（即C-scan）。PAM的纵向分辨率取决于超声探测器的带宽，横向分辨率取决于光焦点或声焦点的大小。根据横向分辨率的决定因素，PAM分为两类：光学分辨率光声显微成像（OR-PAM）和声学分辨率光声显微成像（AR-PAM）。OR-PAM是利用聚焦的激光照射和平场式或聚焦式超声探头探测的，聚焦式探头的检测灵敏度高于非聚焦探头，横向分辨率取决于光学焦斑尺寸，可以达到几微米甚至几百纳米，成像深度约为1 mm，能在细胞和亚细胞尺度成像，对有较强光吸收体的组织成像时对比度较大[6,33-36]。OR-PAM可以工作在透射模式或反射模式下，如图2（a）和图2（b）所示。透射模式通常只适用于较薄的生物样品，反射模式在活体成像中更为方便与实用。为了便于光焦点和声焦点的同轴对准，反射式OR-PAM通常使用由两个棱镜组成的光声耦合器，棱镜之间有硅油层，实现激光透射和超声反射；此外，也可以用薄的盖玻片代替光声耦合器[37]。AR-PAM是

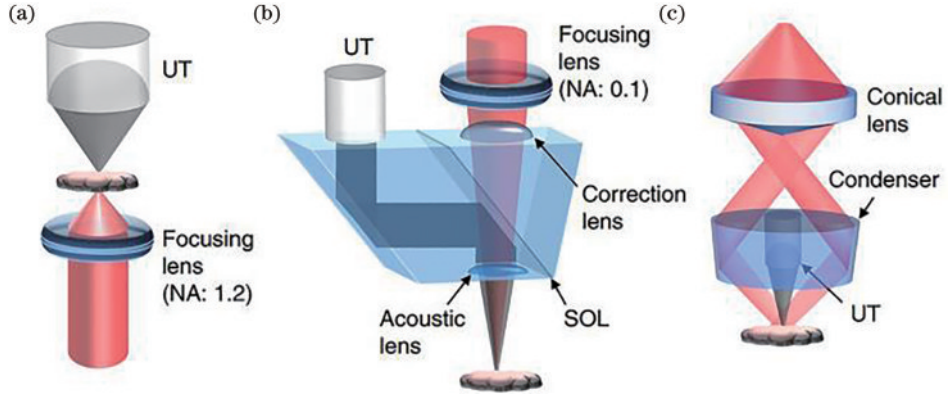

图2 PAM的基本实现方式。（a）透射式OR-PAM[30,35]；（b）反射式OR-PAM[30,36]；（c）基于暗场照明的AR-PAM[30,39]

Fig. 2 Basic implementation of PAM. (a) Transmissive OR-PAM[30,35]; (b) reflective OR-PAM[30,36]; (c) AR-PAM based on dark field illumination[30,39]

利用非聚焦的激光照射和聚焦式超声探头探测的，如图 2(c)所示，成像深度较大(通常为 2～3 mm)，横向分辨率取决于声焦尺寸[38-40]。在高分辨率成像方面，利用光学聚焦的 OR-PAM 优于 AR-PAM，因为光学焦点通常比声学焦点更紧密，而利用声聚焦的 AR-PAM 在穿透深度上比 OR-PAM 更有优势。

PAM 可以利用内源性或外源性造影剂进行生物医学成像研究。图 3 展示了 PAM 的部分结构与功能成像结果。对于内源性造影剂，最常见的是血红蛋白，血红蛋白作为血液中含量最丰富的蛋白质和主要的氧载体，已被 PAM 广泛用于获取血氧饱和度、总血红蛋白浓度和血流速度等多项参数。微血管功能与代谢信息有助于对肿瘤、血管损伤等病变的诊断[41-43]。黑色素在紫外与可见光波段有很高的光吸收，从而作为理想造影剂用于光声监测黑色素瘤，这有助于对皮肤癌及眼病的诊断与监测[44-47]。在近红外区，利用脂质对光的吸收差异可以观测动脉粥样硬化斑块[48-49]，利用光声光谱对葡萄糖浓度进行测量可以为糖尿病的诊断和治疗提供参考[50-51]。此外，有机染料、纳米颗粒及荧光蛋白等外源性造影剂也有助于对深层血管及脑肿瘤等的光声成像[52-56]。

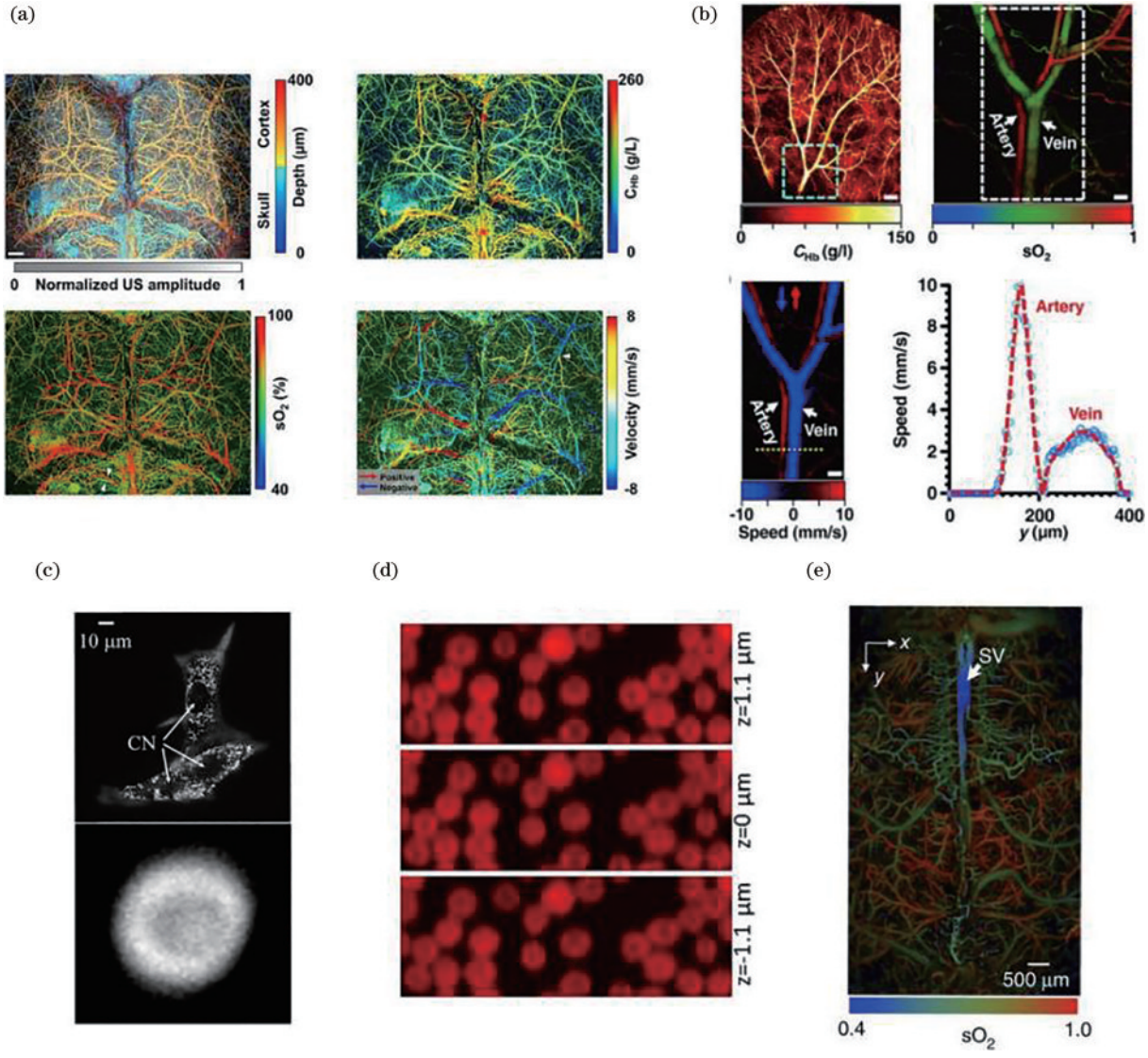

图 3　PAM 结构与功能成像。(a)小鼠大脑多参数测量[57]；(b)小鼠耳部多参数测量[41]；(c)离体黑色素瘤细胞与红细胞成像[35,58]；(d)不同深度血红蛋白观测[59]；(e)小鼠大脑血氧饱和度分布[60]

Fig. 3　Structural and functional imaging of PAM. (a) Multi-parameter measurement of the mouse brain[57]; (b) multi-parameter measurement of the mouse ear[41]; (c) imaging of an *in vitro* melanoma cell and a red blood cell[35,58]; (d) observation for hemoglobin at different depths[59]; (e) distribution of the blood oxygen saturation in a mouse brain[60]

3　便携式光声显微成像的进展

3.1　手持与半手持式

扫描机制的选择是决定 PAM 成像速度、稳定性及小型化的关键。将讨论基于不同扫描设备的手持式与半手持式 PAM 系统。

电控位移台扫描是 PAM 系统传统的扫描方式[6,35,41,61-63]，早期大多 PAM 系统体积庞大，部分研究

者开发了小型化的成像系统。2007年，Maslov等[64]开发了一种便携式实时PAM系统，探头构成如图4(a)所示，系统采用最大重复频率可达2 kHz的可调谐激光器、电控位移台与轻型手持式探头，探头可以放在感兴趣的区域上，能够在不到1 s的时间内获得一个B-scan图像。图4(b)是利用该系统对皮肤不同部位进行探测的截面光声图样。该系统的最大成像深度为5 mm，横向分辨率优于100 μm，轴向分辨率为35 μm。2014年，该小组[65]研究了一种由激光光纤束、聚焦式超声探头与二维线性位移台组成的手持式AR-PAM系统，并对活体裸鼠厚度为3.75 mm的黑色素瘤进行成像观测。探头组成如图4(c)所示，成像结果如图4(d)所示。该系统的分辨率较低(横向分辨率为230 μm，轴向分辨率为59 μm)。2013年，Zeng等[66]开发了一种基于激光二极管的便携式OR-PAM系统，如图4(e)所示，该系统采用线性位移台进行扫描，可以实现1.5 μm的系统横向分辨率，具有结构设计紧凑、成本低廉的优势，但成像速度与稳定性受限。基于该系统，分别对缺损碳纤维表层与嵌入脂肪的深层碳纤维进行了探测成像，结果如图4(f)所示。

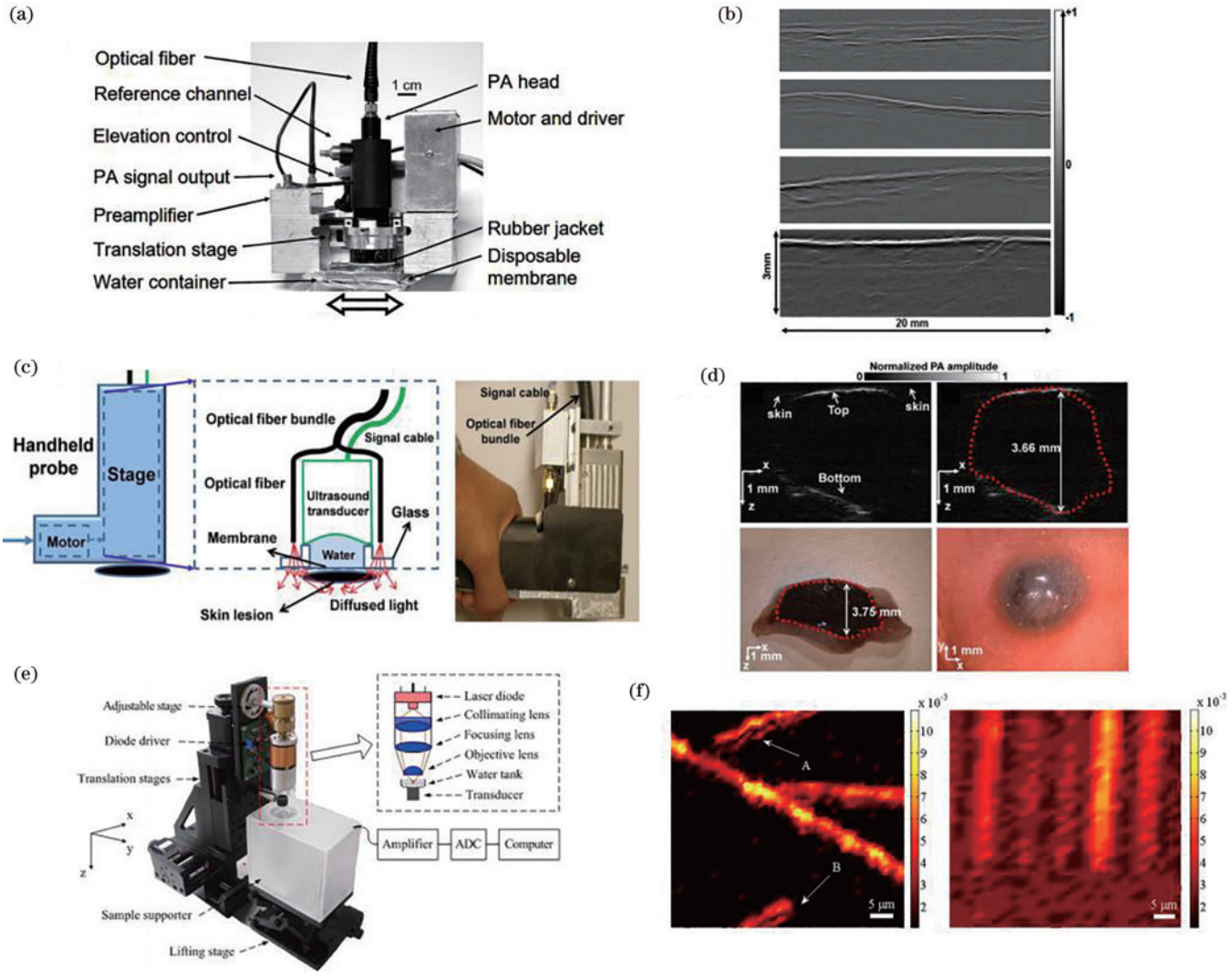

图4 基于电控位移台的便携式PAM。(a)快速扫描PAM探头实物图[64]；(b)人体皮肤不同部位的截面光声图样[64]；(c)基于光纤束照明的AR-PAM，包括探头装置原理图与实物图[65]；(d)裸鼠体内黑色素瘤成像[65]；(e)基于激光二极管的OR-PAM装置图[66]；(f)缺损碳纤维表层与嵌入脂肪的深层碳纤维成像[66]

Fig. 4 Portable PAM based on electronically controlled displacement stage. (a) Photograph of fast scanning PAM probe[64]; (b) cross-sectional photoacoustic patterns of different parts of human skin[64]; (c) AR-PAM based on fiber bundle illumination, including schematic diagram and physical map of the probe device[65]; (d) melanoma imaging in a nude mouse[65]; (e) diagram of OR-PAM device based on laser diode[66]; (f) imaging of the defective carbon fiber surface layer and deep carbon fiber embedded in fat[66]

体积较大的步进电机通常难以实现小、轻、快的成像设备。为了提升系统成像性能与扫描速度，各种新型高速扫描技术进入了人们的视野。音圈扫描是实现高速PAM技术的方式之一[67-69]。然而，音圈扫描的速度从根本上受限于音圈的驱动力和扫描头的质量，考虑长期工作的稳定性，不易于集成化发展。近年来，已

经开发出许多稳定灵活的扫描镜，极大提升扫描速度。检流计式扫描(GS)振镜和微机电系统(MEMS)振镜是两种关键的扫描实现方式。GS振镜的尺寸较大，对激光光束的扫描范围大，在空气中使用稳定性较好，但由于声焦区域是有限的，光束和声束之间难以实现同轴对准，视场大易造成离焦。因此，系统大多采用非聚焦超声换能器来检测信号，但存在灵敏度较低、分辨率不稳定的问题。MEMS振镜的尺寸较小，轻便灵活，更易于集成化与便携化。水浸式的MEMS振镜可以同时扫描光束与声束，结合聚焦式超声换能器检测信号，实现光-声共聚焦，具有均匀的探测灵敏度与较高的成像信噪比。但有限的声焦区域限制了其成像视场基本在3 mm以内。表1给出了GS振镜与MEMS振镜用于便携化光声显微成像系统的成像性能与发展情况比较。

表1 GS振镜与MEMS振镜的成像性能比较

Table 1 Comparison of the imaging performance of GS mirror and MEMS mirror

Scanner type	Reference	System size	Imaging speed /Hz (B-scan)	Imaging range	Lateral resolution / μm	Demonstration
GS mirror	[70]	40 mm×60 mm	800	800 μm	7	*in vivo* mouse ear
	[71]	–	25	2 mm×2 mm	8.9	*in vivo* rooster's wattle, human lip, and wrist
	[72]	~100 cm×180 cm	25	14.5 mm×9 mm	11.5	*ex vivo* chicken breast tissue, *in vivo* mouse ear, iris, and brain
	[73-74]	–	10	8.5 mm×1.5 mm	10.4, 4.2	*in vivo* mouse ear, brain, eyes, and human mouth
	[75]	–	133	10 mm	15	*in vivo* rhesus monkey brain
	[76]	100 mm×130 mm×140 mm	400	10 mm×10 mm	10	*in vivo* mouse brain
	[77]	59 mm × 30 mm × 44 mm	1288	~1.7mm×5 mm	6.2	*in vivo* mouse organs
MEMS mirror	[78]	80 mm × 115 mm × 150 mm	–	2.5 mm × 2 mm	5	*in vivo* mouse ear, human skin
	[79]	diameter ~ 17 mm	35	2.8 mm × 2 mm	12	*in vivo* mouse ear, iris, brain, and human finger
	[80]	60 mm × 30 mm × 20 mm	~31	0.9 mm×0.9 mm	10.4	*in vivo* mouse ear, brain, and human lip
	[37,81]	22 mm × 30 mm × 13 mm	100	2 mm × 2 mm	3.8	*in vivo* mouse ear, abdomen, and human mouth
	[82]	diameter~12 mm	100	2.4 mm	18.2	*in vivo* human mouth

GS振镜具有精度高、速度快、稳定性好等优点，相比于传统的电控位移台，可以减小体积，实现激光束的快速扫描[83-89]。2011年，Hajireza等[70]首次研制了手持式实时OR-PAM，采用由30000根单模光纤组成的光纤束进行引导和GS振镜进行激光扫描，质量约500 g的手持式探头进行探测，获得了小鼠耳部微血管的成像结果。该系统兼具小型化与集成化，占地面积为40 mm×60 mm，但是，光纤束成本较高，成像视场较小，扫描速度慢，从而限制了广泛应用。2019年，Zhang等[71]开发了一种具有可调光焦点的手持式光声探测系统，如图5(a)所示。该系统采用快速的二维GS振镜进行激光扫描，其中的手持式探头可以用于人体嘴唇和人体皮肤微血管成像，如图5(b)所示，获得血管直径和深度等定量信息，具有成像速度快、空间分辨率高、穿透深度深的特点。该光声探头获取2 mm×2 mm(400×400像素)的MAP图像需要16 s，B-scan成像速度为25 frame/s，横向分辨率约为8.9 μm，成像深度约为2.4 mm。2021年，Seong等[72]研制了具有大视场(14.5 mm×9 mm)的手持式PAM装置，如图5(c)所示，并对小鼠组织，包括耳、虹膜和脑进行了体内成像，成像结果如图5(d)所示。系统采用光声耦合器实现光束与声信号的同轴与共聚焦，采用双轴水浸式GS振镜对激光进行快速扫描，其中的探头可以根据样品形状与大小进行自由移动调节。除了栅格式的扫描，基于旋转扫描的PAM具有大视场、高时间分辨率的优势。Jin等[73-75]首次开发了基于旋转扫描的便携式OR-PAM系统，系统装置如图5(e)所示，采用二维GS振镜进行快速光学扫描，电控旋转聚焦式超声换能器将声焦线调整为与光学成像平面共聚焦。该系统一方面能够对中小型动物和人类口腔进行结构成像，另一方面可用于观测脑神经活动。图5(f)是对小鼠肿瘤的血管发展进行监测得到的图样。在低分辨率与高分辨率两种模式下，系统的横向分辨率分别为10.8 μm与4.2 μm，轴向分辨率分别为90 μm与60 μm。2021年，同组的Qin等[76]通过使用具有较长工作距离的新型光学系统、较高脉冲重复频率的激光源

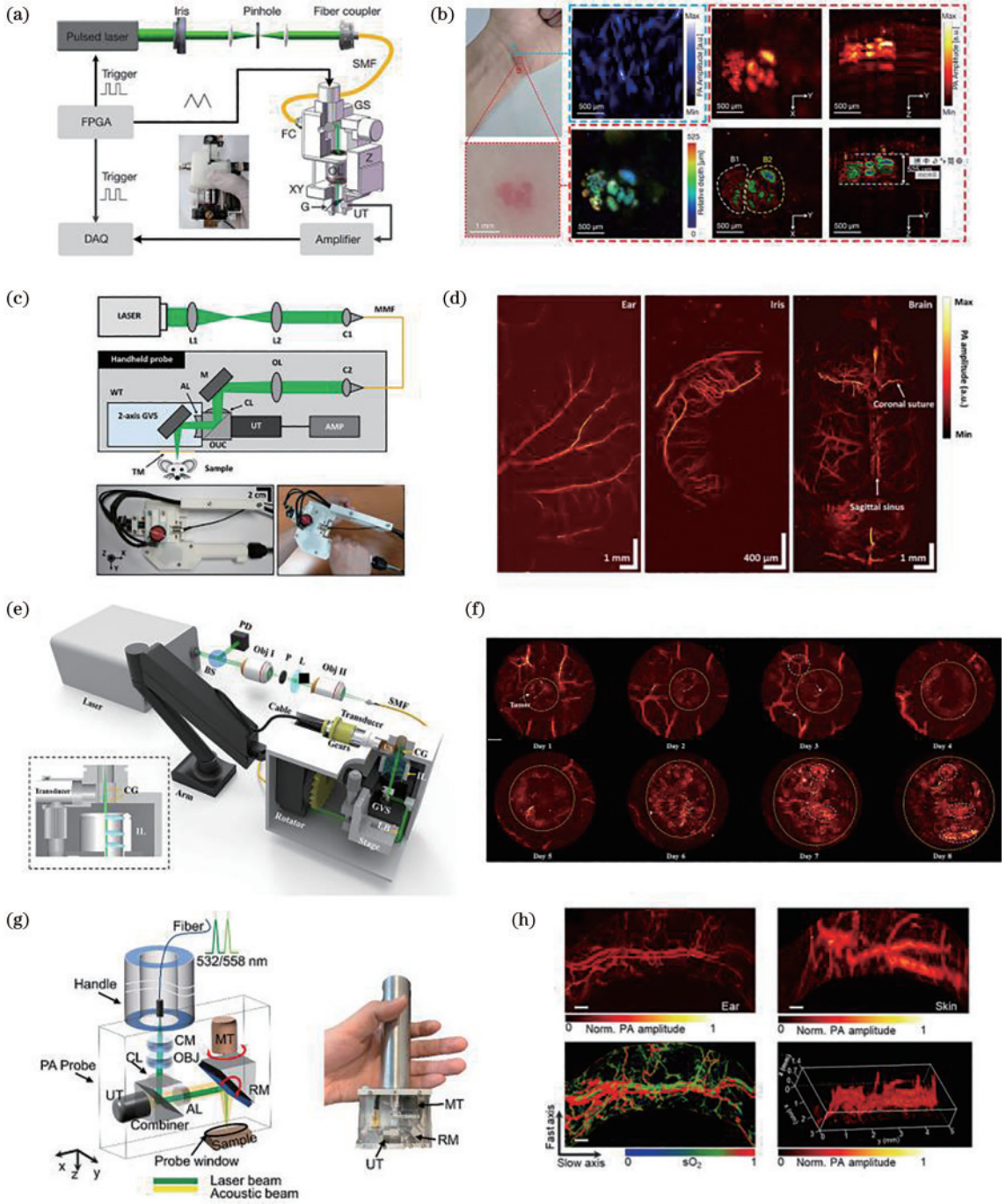

图 5 采用 GS 振镜扫描的便携式 PAM。(a)可调光焦点的 PAM 系统原理图与探头实物图[71];(b)人体手腕部位皮下血管成像[71];(c)具有大视场的 PAM 系统原理图与探头实物图[72];(d)小鼠耳部、虹膜及脑部微血管成像[72];(e)基于旋转扫描的 PAM 系统装置图[73];(f)小鼠肿瘤的血管变化监测[73];(g)混合扫描的 PAM 装置原理图与实物图[77];(h)小鼠耳部与背部的血管及血氧图样[77]

Fig. 5 Portable PAM using GS galvanometer scanning. (a) PAM system schematic with adjustable light focus and the physical picture of the probe[71]; (b) imaging of subcutaneous blood vessels at the human wrist[71]; (c) schematic of PAM system with large field-of-view and physical picture of the probe[72]; (d) imaging of the mouse ear, iris, and brain microvessels[72]; (e) schematic of PAM system based on the rotational scanning[73]; (f) monitoring of vascular changes in a mouse tumor[73]; (g) schematic and photograph of the PAM device with hybrid scanning[77]; (h) vessels and oxygen saturation images of the mouse ear and back[77]

和具有精确定位功能的自动机械臂进一步改进了系统。新系统的时间分辨率为 5 s,横向和轴向空间分辨率分别为 15 μm 与 120 μm,横向成像视场为 10 mm。研究人员分析了在缺氧状态下恒河猴脑血管的结构和功能反应。2022 年,Chen 等[77]提出了一种利用微型旋转电机和 GS 振镜混合扫描的手持式 PAM 系统,如图 5(g)所示,系统的 B-scan 速度达到 1288 Hz,可以实现灵活、高速的三维成像。利用该系统分别对小鼠不

同部位进行了血管成像与血氧饱和度探测，结果如图 5(h)所示。

相比于GS振镜的扫描方式，MEMS振镜的体积更小，易于集成，有利于PAM系统的进一步小型化与便携化。近些年，将MEMS振镜用于PAM激光扫描有了一系列的研究和发展[60,90-94]，并且多种便携式PAM装置相继被提出，并在生物与人体成像中发挥出巨大的潜力。2017年，Lin等[78]将水浸式MEMS振镜用在手持式OR-PAM中，系统装置如图6(a)所示，该系统利用光声共聚焦扫描来优化信噪比，探头的体积为80 mm×115 mm×150 mm，在样品体积为2.5 mm×2 mm×0.5 mm下的成像速率为2 Hz，横向与轴向空间分辨率分别为5 μm与26 μm。通过对小鼠耳部血管与人体皮肤的测试，验证了该装置的灵活性与有效性。图6(b)是用该装置对人体手臂部位进行探测成像的过程图与成像结果。2017年，Park等[79]研发了一种质量为162 g、直径为17 mm的手持式集成光声探头，如图6(c)所示，系统采用水浸式MEMS振镜实现光声扫描，并采用小型化平面超声换能器实现超声信号探测，通过使用50 kHz脉冲激光，获取700×700像素的图像所需的B-scan和体积成像速度分别为35 Hz和0.05 Hz，系统横向和轴向分辨率分别为12 μm和30 μm。基于该系统，实验人员分别测得了图6(d)所示的活体小鼠耳朵、虹膜和大脑微血管的高分辨率图像，以及人体手指上痣的图像。基于MEMS振镜扫描，Xi小组[37,80-81]分别研制了探头体积为60 mm×30 mm×20 mm和质量为40 g、探头体积为22 mm×30 mm×13 mm和质量为20 g的手持式OR-PAM系统，用于对小型动物及人体的体内成像观测，优化后的系统可以提供0.2 Hz的帧速率、2 mm×2 mm的视场、3.8 μm的横向分辨率和104 μm的轴向分辨率。利用研发的系统，该团队分别对小鼠不同部位及人体口腔等血管进行了成像，捕获了毛细血管中的红细胞流动，监测了出血和输注过程中的血管变化等。图6(e)是该探头的构成示意图与实物图，图6(f)是部分成像结果。2020年，Zhang等[82]研发了一种手持式的光声笔，如图6(g)所示，该装置具有4 frame/s的高速成像模式和0.25 frame/s的高分辨率成像模式，其横向分辨率为18.2 μm，轴向分辨率为137.4 μm，图6(h)是利用该光声笔对口腔微血管进行成像的结果。

3.2 脑部可穿戴式

大脑作为人体重要且复杂的生命器官，起着统筹和调控的作用，主导机体的生命活动。对大脑神经活动与血液微环境的监测有助于及早发现与诊断脑部疾病。目前，多种脑影像技术已用于临床诊断，并发挥着重要作用，比如X射线成像、电子计算机断层扫描成像、正电子发射计算机断层显像技术、磁共振成像以及荧光显微成像等。PAI因高分辨率、大探测深度、无损伤与无需外源性标记等优点可用于脑成像研究中，不同的研究团队对此进行了一系列的研究，从动物到人类，获得了脑血管结构形态特征以及血氧、血流等功能信息[95-102]。

当前的手持式PAM仍具有体积大、质量大、无法实现可穿戴脑成像等问题，发展小型、轻便的可穿戴式脑监测技术可以更加灵活准确地了解大脑结构和功能性活动。Cao等[103-105]提出了一种基于悬浮球和头部固定装置的PAM系统，如图7(a)和图7(b)所示，分别对清醒与麻醉的小鼠大脑进行了结构和功能成像，并比较了不同麻醉深度下的反应。随后，他们研究了高脂肪饮食引起的肥胖小鼠模型的脑血管改变，同时基于深度学习，利用算法去除混响伪影，优化深度分辨信号。2021年，该小组[106]设计了一种轻量级(2 g)、宽视场(5 mm×7 mm)的头戴式颅窗，如图7(c)所示，通过对小鼠在清醒与麻醉状态下的脑血管结构、功能及氧代谢进行成像，以及监测缺血性脑卒中小鼠脑血管的变化，证明了该多参数PAM系统的实用性。

此外，Xi等[107]在2017年提出了一种适用于自由运动大鼠神经血管单点成像的探针，图7(d)是探测图，该探针将光声传感器和微电极集成到一个微型装置中，可以用于观察单根血管的血流动力学和神经活动的情况。2019年，该小组[108]开发了一个质量为8 g、直径为13 mm的小型PAM探针，如图7(e)所示，该探头集成了一个光学旋转接头和一个定制的电滑环来传递激发光和传输电信号，系统的横向分辨率达到2.25 μm，具有高时空分辨率、大视场、易于组装和光学焦距可调等特点。通过将该系统安装在小鼠头部，监测了自由运动小鼠在缺血再灌注诱导过程中大脑皮层血管的形态和功能的变化。2020年，Dangi等[109]设计了一种低成本、可穿戴式的PAM系统，该系统由直径为2.5 mm的环形超声换能器、光纤耦合激光二极管和小型化平移台集成，如图7(f)所示。但是，该系统的有效性只在仿体得到了初步验证。2021年，Guo等[110]设计了质量为1.8 g、具有约3 mm×3 mm大视场的头戴式探头，并将其用于自由运动小鼠脑成像。

3.3 集成多模态

新的成像技术不断发展，为获取有价值的功能和形态信息开辟了新的途径。每一种成像方式都有特定的优势和内在的局限性，为了补偿不同模态的不足，多模态成像技术的研究已成为生物医学和临床应用的一种趋势。它结合了不同成像模式的优势和互补能力，与单一模式相比，可以提供更全面的组织诊断。目前，针对不同的应用，研究者已提出多种结合光声成像的多模态成像技术，并将技术用于对生物组织结构与功能信息的探测，如皮肤、视网膜和口腔等[111-120]。为了克服时间分辨率低、体积大、视场小及难以用于人体等限制，研究者开发了小型化集成多模态的系统。

PAM和共聚焦荧光显微成像(CFM)可以分别在薄光学切片内实现对微血管和细胞结构的高分辨率成

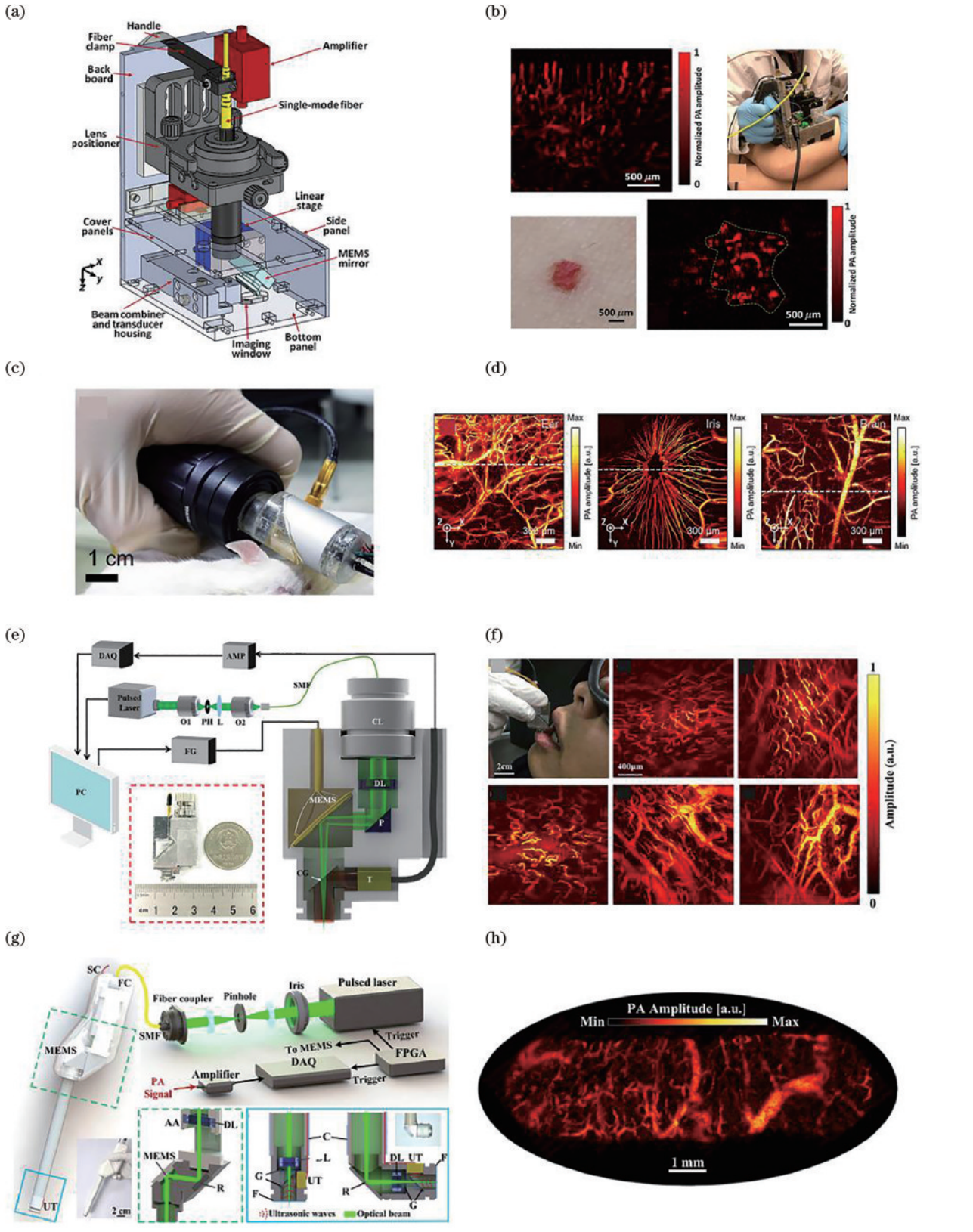

图 6 采用 MEMS 振镜扫描的便携式 PAM。(a)紧凑设计的手持式 PAM 系统示意图[78];(b)人体皮肤血管成像[78];(c)质量为 162 g、直径为 17 mm 的光声探头实物[79];(d)小鼠耳部、虹膜及脑部血管成像[79];(e)体积为 22 mm×30 mm×13 mm、质量为 20 g 的探头装置[37];(f)人体口腔血管成像[37];(g)光声笔的装置[82];(h)人体口腔血管成像[82]

Fig. 6 Portable PAM using MEMS galvanometer scanning. (a) Diagram of the compactly designed handheld PAM system[78]; (b) imaging of human skin vessels[78]; (c) photograph of a photoacoustic probe with a mass of 162 g and a diameter of 17 mm[79]; (d) imaging of mouse ear, iris, and brain vessels[79]; (e) diagram of the probe with a volume of 22 mm×30 mm×13 mm and a mass of 20 g[37]; (f) imaging of human oral vessels[37]; (g) diagram of the photoacoustic pen[82]; (h) imaging of human oral vessels[82]

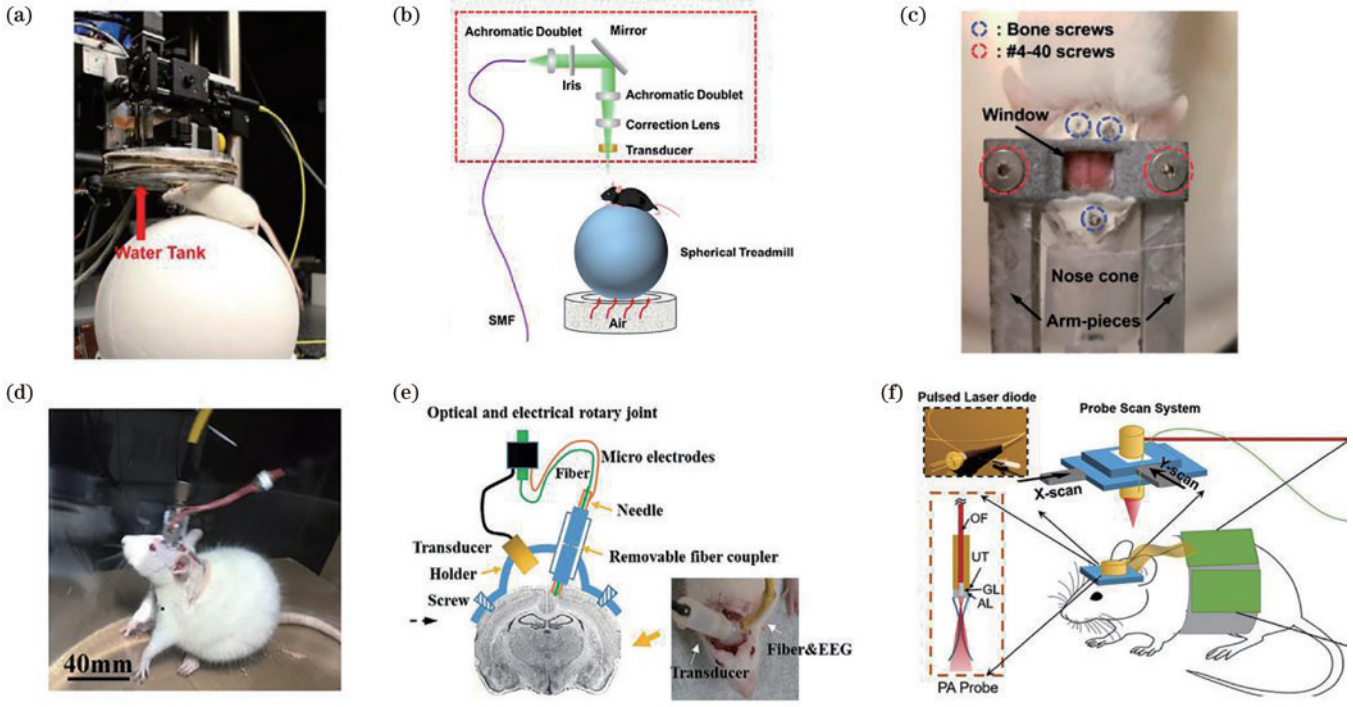

图 7 脑部可穿戴式的 PAM。(a)(b)基于悬浮球和头部固定装置的部分实物与原理[103-104];(c)轻量级(2 g)、宽视场(5 mm×7 mm)的头戴式颅窗实物[106];(d)用于自由运动大鼠神经活动监测的装置[107];(e)质量为 8 g、直径为 13 mm 的小型脑部探针[108];(f)低成本与小型化系统示意图[109]

Fig. 7 Wearable PAM for the brain. (a) (b) Partial photograph and schematic diagram based on the suspended ball and head fixation device[103-104]; (c) photograph of the head-mounted cranial window with mass of 2 g and wide field-of-view of 5 mm×7 mm[106]; (d) device for monitoring neural activity in freely moving rat[107]; (e) small brain probe with mass of 8 g and diameter of 13 mm[108]; (f) schematic of the low-cost and miniaturized system[109]

像。这两种成像技术都可以通过光学聚焦实现,并提供微米级分辨率的体内成像。PAM 与 CFM 结合的双模态系统能进行双分子对比成像,提供更全面的诊断信息[120-122]。2013 年,Chen 等[123]开发了一种结合 PAM 与 CFM 的双模态小型化系统,如图 8(a)所示,系统采用了微型元件,包括 MEMS 振镜、微型物镜和小型声探测器。PAM 和 CFM 具有相同的激光源和扫描光路,分别激发光声信号和荧光信号。PAM 和 CFM 的横向分辨率均为 8.8 μm。PAM 和 CFM 的轴向分辨率分别为 19 μm 和 53 μm。基于该系统对离体动物膀胱组织进行了实验,成像结果如图 8(b)所示。目前,基于 PAM 与 CFM 双模态的便携化系统还相对较少,未来有望进一步研发。

光学相干层析成像(OCT)是一种具有高分辨率的光学成像技术。与光声成像不同,OCT 是基于相干测量原理的,从组织内部微结构的光散射中获得成像对比度[124-126]。将具有高空间分辨率的 OCT 和 PAM 结合,可以获得精细血管结构和亚细胞特征,促进脑疾病的诊断[127-131]。Xi 等[132-134]开发了一系列结合 OR-PAM 和 OCT 的小型化系统,分别对小鼠耳部、人体口腔等进行成像,并监测口腔溃疡的恢复进展,如图 8(c)~(f)所示。系统的横向分辨率可达 3.7 μm(OR-PAM)和 5.6 μm(OCT),尺寸为 65 mm×30 mm×18 mm,质量为 35.4 g。

除了 PAM 与 OCT 结合的双模态系统,超声(US)成像可以获取深层组织结构,具有大深度探测的特点,并且一个通用的超声换能器可以同时用于 US 和 PAM 探测,将 PAM 与 US 成像技术结合可以同时获取深层组织与浅层组织信息[135-138]。2014 年,Daoudi 等[139]研究了一种手持式 PA/US 双模态成像系统,通过对人体手指关节的成像,验证了该系统良好的成像速度与成像深度,在 0.5 Hz 帧率下穿透深度达到 15 mm。但是,由于系统不是用聚焦的激光照射,导致分辨率不佳,达到几百微米。同年,Bai 等[135]研发了一种用于血管内成像的光声-超声探针,探针直径仅有 1.1 mm,该系统的横向分辨率达 19.6 μm,比传统的血管内光声成像和超声成像精细 10 倍。利用该系统对仿体进行了双模态并行成像,获取了互补的结构和深度信息。

将 PAM、US、OCT 三模态结合,可以充分利用不同模态的成像优势,提供生物组织的光学吸收、光学后向散射和深层组织结构等互补信息[118,140-143]。2015 年,Dai 等[144]提出了一种三模态微型侧视探头,如图 8(g)所示,探头直径为 2 mm。利用该集成探针,获取了活体小鼠耳部血管的三模态成像,如图 8(h)所示。该探针在 OR-PAM 和 OCT 模态下的横向分辨率为

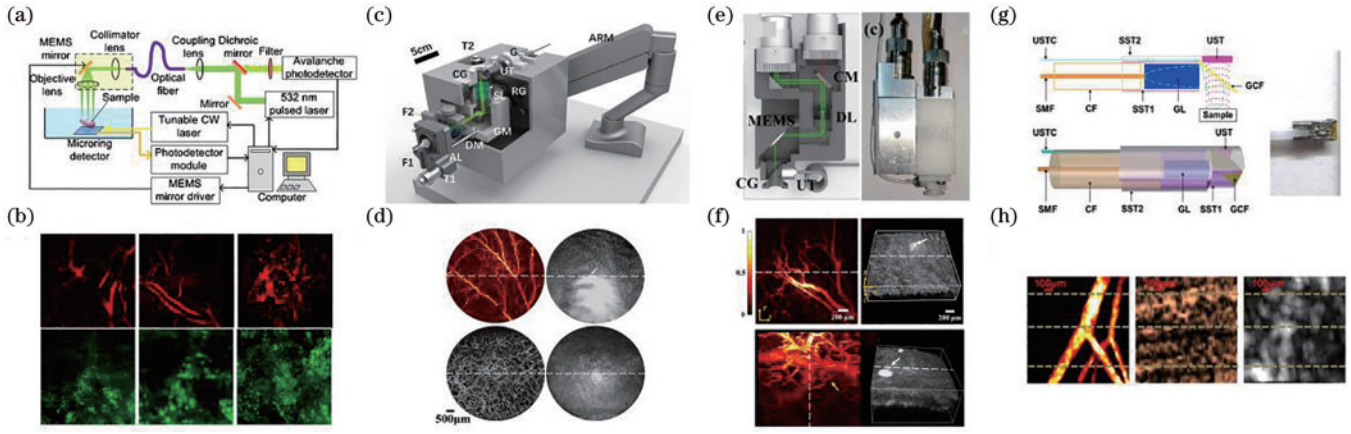

图 8　基于多模态的小型化 PAM。(a)结合 PAM 与 CFM 的双模态系统原理[123]；(b)动物膀胱组织的 PAM(上排)与 CFM(下排)成像[123]；(c)基于旋转扫描的 OR-PAM 与 OCT 双模态系统装置[132]；(d)小鼠耳部(上排)与人体下唇(下排)的 OR-PAM 与 OCT 成像[132]；(e)质量为 35.4 g、体积为 65 mm×30 mm×18 mm 的 OR-PAM 与 OCT 双模态探头结构与实物[133]；(f)小鼠耳部(上排)及人体口腔下唇(下排)的 OR-PAM 与 OCT 成像[133]；(g)PAM-US-OCT 三模态探针原理及实物[144]；(h)小鼠耳部血管 PAM(左)、US(右)、OCT(中)三模态成像[144]

Fig. 8　Miniaturized PAM based on multi-modality. (a) Schematic of a dual-modality system combining PAM and CFM[123]; (b) PAM (upper row) and CFM (lower row) imaging of animal bladder tissue[123]; (c) device diagram of OR-PAM and OCT dual-modality system based on rotary scanning[132]; (d) OR-PAM and OCT imaging of mouse ear (upper row) and human lower lip (lower row)[132]; (e) structure and photograph of the OR-PAM and OCT dual-modality probe with a mass of 35.4 g and a volume of 65 mm×30 mm×18 mm[133]; (f) OR-PAM and OCT imaging of mouse ear (upper row) and human oral lower lip (lower row)[133]; (g) schematic diagram and photograph of PAM-US-OCT three-modality probe[144]; (h) PAM (left), US (right), and OCT (medium) three-modality imaging of mouse ear blood vessels[144]

13.4 μm，在 OR-PAM 和 US 模态下的轴向分辨率为 43 μm。2017 年，同一小组[145]将 PAM-US-OCT 三模态集成到基于双包层光纤的单个探头中，探头的直径减小到 1 mm。利用该探针，分别对小鼠耳部、人的手部和有动脉粥样硬化斑块的血管进行了三模态成像。2021 年，Leng 等[146]开发了一种结合 PA、US 与 OCT 的微型成像系统，获取了血管壁的宏观和微观结构信息，并利用光声光谱进行了脂质组成鉴定和脂质浓度分布分析。该系统通过利用直径仅为 0.9 mm 的细导管，可以在血管内实现 360°连续旋转和拉回。

4　面临的挑战

经过二十多年的发展，光声成像已成为医学成像领域的重要研究手段。PAM 作为光声成像的重要分支，在空间分辨率、成像深度、成像速度、信号探测及便携化等方面得到了快速发展，目前已广泛应用于动物及人体的结构、功能与分子成像。为了促进临床转化，满足不同的基础应用，轻量化、体积小的便携化设备必然是未来 PAM 发展的趋势之一[147-151]。但是，未来仍面临着一些挑战。1)大多数 PAM 系统通过一个激光脉冲获取一维深度分辨的光声信号，需要多次点对点二维扫描重建图像，难以实时显示宽视场图像。对于手持式探头，往往需要在一个区域完成扫描成像后再移到另一个区域，这限制了成像速度，增加了临床应用的诊断时间，这对研发高速与大视场设备提出了要求。一方面，可以探索利用微透镜阵列实现平行扫描，缩短扫描时间。另一方面，开发更快的成像技术和信号处理算法，以实现高速成像和实时监测[152]。2)由于光学和声学衰减导致的深度信噪比下降，较深信号的低信噪比可能会阻碍对相对较大组织信息的充分获取。未来可以探索利用深度学习去除伪影[153-158]，提高深层组织图像的信噪比与图像质量。3)大多数 PAM 需要水或超声凝胶等耦合介质填充或涂覆于探头与皮肤组织间，这限制了许多术中应用。使用新型探测设备或许可以克服该问题，与压电传感器相比，光学检测也是可以考虑的[159-164]，同时有利于系统的进一步小型化。4)完全的便携化是不需要复杂的光路系统的，可以直接将探头连接到成像平台进行光传输和信号传输。目前，大多 PAM 系统主要在成像探头部分进行了手持式或便携式考虑，要想实现整个系统小型化，对光学和机械部件的集成提出了挑战，需要找到适当的平衡，保持成像性能的同时满足便携性的需求。5)未来将便携式 PAM 技术应用于临床环境需要考虑医学标准、安全性和患者隐私等问题。相关的法规和标准化工作也需要进一步发展和制定，以确保成像设备的可靠性、准确性和安全性。除了上述挑战之外，可以将便携式 PAM 技术与更多其他互补模态融合，发挥不同模态成像的优势，增强临床适用性。

5 总结与展望

PAM利用高光学吸收对比度，结合低衰减的超声探测，具有三维高分辨率成像能力，可以提供形态、功能和分子信息。近些年，随着成像性能不断被优化，包括空间分辨率、穿透深度、探测灵敏度、成像速度等，PAM已发展成生物医学研究的重要工具，在脑科学、肿瘤、眼科学及神经学等领域获得广泛的研究。为了将其发展为一个有广泛普适性的临床成像平台，小型化体积与便携化设计的PAM是当前研究的热点。本文对便携式PAM的发展情况与研究现状进行了综述。目前的便携式PAM系统在结构设计、外形及使用方式上差异很大，主要研究还停留在实验室，难以被普遍接受和临床应用。随着新技术与人工智能的飞速发展，未来PAM系统有望在集成化、图像处理等方面得到优化。此外，系统研发与用户实际需求要密切结合，结合当前的技术瓶颈，研发能被普遍接受和便于操作的临床成像平台。

总之，便携式PAM技术在医学和生物科学领域具有巨大潜力，随着不断的创新和技术发展，便携式PAM技术会走向成像性能更优、应用范围更广、普适性更高的新阶段。

参 考 文 献

[1] Wang L V, Hu S. Photoacoustic tomography: *in vivo* imaging from organelles to organs[J]. Science, 2012, 335(6075): 1458-1462.

[2] 穆根, 张振辉, 石玉娇. 生物医学影像中的光声成像技术[J]. 中国激光, 2022, 49(20): 2007208.
Mu G, Zhang Z H, Shi Y J. Photoacoustic imaging technology in biomedical imaging[J]. Chinese Journal of Lasers, 2022, 49(20): 2007208.

[3] Wang B, Karpiouk A, Yeager D, et al. Intravascular photoacoustic imaging of lipid in atherosclerotic plaques in the presence of luminal blood[J]. Optics Letters, 2012, 37(7): 1244-1246.

[4] Yang J G, Choi S, Kim J, et al. Recent advances in deep-learning-enhanced photoacoustic imaging[J]. Advanced Photonics Nexus, 2023, 2(5): 054001.

[5] Zhang Z H, Chen W, Cui D D, et al. Collagen fiber anisotropy characterization by polarized photoacoustic imaging for just-in-time quantitative evaluation of burn severity[J]. Photonics Research, 2023, 11(5): 817-828.

[6] Maslov K, Zhang H F, Hu S, et al. Optical-resolution photoacoustic microscopy for in vivo imaging of single capillaries[J]. Optics Letters, 2008, 33(9): 929-931.

[7] Yao J J, Wang L D, Li C Y, et al. Photoimprint photoacoustic microscopy for three-dimensional label-free subdiffraction imaging[J]. Physical Review Letters, 2014, 112(1): 014302.

[8] Shi J H, Wong T T W, He Y, et al. High-resolution, high-contrast mid-infrared imaging of fresh biological samples with ultraviolet-localized photoacoustic microscopy[J]. Nature Photonics, 2019, 13: 609-615.

[9] Yang J M, Gong L, Xu X, et al. Motionless volumetric photoacoustic microscopy with spatially invariant resolution[J]. Nature Communications, 2017, 8: 780.

[10] Cao R, Zhao J J, Li L, et al. Optical-resolution photoacoustic microscopy with a needle-shaped beam[J]. Nature Photonics, 2023, 17: 89-95.

[11] Zhang X, Li Z L, Nan N, et al. Super-resolution reconstruction algorithm for optical-resolution photoacoustic microscopy images based on sparsity and deconvolution [J]. Optics Express, 2023, 31(1): 598-609.

[12] Lee S Y, Lai Y H, Huang K C, et al. *In vivo* sub-femtoliter resolution photoacoustic microscopy with higher frame rates[J]. Scientific Reports, 2015, 5: 15421.

[13] Wong T T W, Zhang R Y, Hai P F, et al. Fast label-free multilayered histology-like imaging of human breast cancer by photoacoustic microscopy[J]. Science Advances, 2017, 3(5): e1602168.

[14] Li X F, Kot J C K, Tsang V T C, et al. Ultraviolet photoacoustic microscopy with tissue clearing for high-contrast histological imaging[J]. Photoacoustics, 2022, 25: 100313.

[15] Cao R, Nelson S D, Davis S, et al. Label-free intraoperative histology of bone tissue via deep-learning-assisted ultraviolet photoacoustic microscopy[J]. Nature Biomedical Engineering, 2023, 7: 124-134.

[16] Wang Z Y, Yang F, Cheng Z W, et al. Photoacoustic-guided photothermal therapy by mapping of tumor microvasculature and nanoparticle[J]. Nanophotonics, 2021, 10(12): 3359-3368.

[17] Staley J, Grogan P, Samadi A K, et al. Growth of melanoma brain tumors monitored by photoacoustic microscopy[J]. Journal of Biomedical Optics, 2010, 15(4): 040510.

[18] 孙彤, 黄国家, 张振辉. 基于高分辨光声显微成像的肝癌微血管特征分析[J]. 中国激光, 2023, 50(15): 1507105.
Sun T, Huang G J, Zhang Z H. Characteristics analysis of micro-vessels liver cancer based on high resolution photoacoustic microscopy[J]. Chinese Journal of Lasers, 2023, 50(15): 1507105.

[19] Liu C, Chen J B, Zhang Y C, et al. Five-wavelength optical-resolution photoacoustic microscopy of blood and lymphatic vessels[J]. Advanced Photonics, 2021, 3(1): 016002.

[20] Xu Z Q, Pan Y H, Chen N B, et al. Visualizing tumor angiogenesis and boundary with polygon-scanning multiscale photoacoustic microscopy[J]. Photoacoustics, 2022, 26: 100342.

[21] Chang K W, Zhu Y H, Hudson H M, et al. Photoacoustic imaging of squirrel monkey cortical and subcortical brain regions during peripheral electrical stimulation[J]. Photoacoustics, 2022, 25: 100326.

[22] Liao L D, Li M L, Lai H Y, et al. Imaging brain hemodynamic changes during rat forepaw electrical stimulation using functional photoacoustic microscopy[J]. NeuroImage, 2010, 52(2): 562-570.

[23] He Y, Shi J H, Maslov K I, et al. Wave of single-impulse-stimulated fast initial dip in single vessels of mouse brains imaged by high-speed functional photoacoustic microscopy[J]. Journal of Biomedical Optics, 2020, 25(6): 066501.

[24] Jeon S, Song H B, Kim J, et al. *In vivo* photoacoustic imaging of anterior ocular vasculature: a random sample consensus approach[J]. Scientific Reports, 2017, 7: 4318.

[25] Zhang W, Li Y X, Nguyen V P, et al. Ultralow energy photoacoustic microscopy for ocular imaging in vivo[J]. Journal of Biomedical Optics, 2020, 25(6): 066003.

[26] Zhao H X, Li K, Yang F, et al. Customized anterior segment photoacoustic imaging for ophthalmic burn evaluation in vivo[J]. Opto-Electronic Advances, 2021, 4(6): 200017.

[27] Hattori H, Namita T, Kondo K, et al. Study for evaluation of skin aging with photoacoustic microscopy [J]. Proceedings of SPIE, 2020, 11240: 112400C.

[28] Favazza C, Jassim O W, Wang L V, et al. *In vivo* photoacoustic microscopy of human skin[J]. Journal of Investigative Dermatology, 2010, 130(S1): S145.

[29] Bell A G. On the production and reproduction of sound by light[J]. American Journal of Science, 1880, 20(118): 305-324.

[30] Wang L V, Yao J J. A practical guide to photoacoustic tomography in the life sciences[J]. Nature Methods, 2016, 13: 627-638.

[31] Oraevsky A A, Jacques S L, Esenaliev R O, et al. Laser-based optoacoustic imaging in biological tissues[J]. Proceedings of SPIE, 1994, 2134: 122-128.

[32] Manwar R, Zafar M, Xu Q Y. Signal and image processing in biomedical photoacoustic imaging: a review [J]. Optics, 2020, 2(1): 1-24.

[33] Hu S, Maslov K, Wang L V. Second-generation optical-resolution photoacoustic microscopy with improved sensitivity and speed[J]. Optics Letters, 2011, 36(7): 1134-1136.

[34] Chen M M, Jiang L M, Cook C, et al. High-speed wide-field photoacoustic microscopy using a cylindrically focused transparent high-frequency ultrasound transducer [J]. Photoacoustics, 2022, 28: 100417.

[35] Zhang C, Maslov K, Wang L V. Subwavelength-resolution label-free photoacoustic microscopy of optical absorption *in vivo*[J]. Optics Letters, 2010, 35(19): 3195-3197.

[36] Shintate R, Ishii T, Ahn J, et al. High-speed optical resolution photoacoustic microscopy with MEMS scanner using a novel and simple distortion correction method[J]. Scientific Reports, 2022, 12: 9221.

[37] Chen Q, Guo H, Jin T, et al. Ultracompact high-resolution photoacoustic microscopy[J]. Optics Letters, 2018, 43(7): 1615-1618.

[38] Yao J, Wang L V. Photoacoustic microscopy[J]. Laser & Photonics Reviews, 2013, 7(5): 758-778.

[39] Periyasamy V, Das N, Sharma A, et al. 1064 nm acoustic resolution photoacoustic microscopy[J]. Journal of Biophotonics, 2019, 12(5): e201800357.

[40] Fang C, Zou J. Acoustic-resolution photoacoustic microscopy based on an optically transparent focused transducer with a high numerical aperture[J]. Optics Letters, 2021, 46(13): 3280-3283.

[41] Yao J J, Maslov K I, Zhang Y, et al. Label-free oxygen-metabolic photoacoustic microscopy in vivo[J]. Journal of Biomedical Optics, 2011, 16(7): 076003.

[42] Sun N D, Zheng S Q, Rosin D L, et al. Development of a photoacoustic microscopy technique to assess peritubular capillary function and oxygen metabolism in the mouse kidney[J]. Kidney International, 2021, 100(3): 613-620.

[43] Sun N D, Bruce A C, Ning B, et al. Photoacoustic microscopy of vascular adaptation and tissue oxygen metabolism during cutaneous wound healing[J]. Biomedical Optics Express, 2022, 13(5): 2695-2706.

[44] Fakhoury J W, Lara J B, Manwar R, et al. Photoacoustic imaging for cutaneous melanoma assessment: a comprehensive review[J]. Journal of Biomedical Optics, 2024, 29(S1): S11518-S11518.

[45] Cho S W, Phan T T V, Nguyen V T, et al. Efficient label-free *in vivo* photoacoustic imaging of melanoma cells using a condensed NIR-I spectral window[J]. Photoacoustics, 2023, 29: 100456.

[46] Chen H Y, Agrawal S, Dangi A, et al. Optical-resolution photoacoustic microscopy using transparent ultrasound transducer[J]. Sensors, 2019, 19(24): 5470.

[47] Galanzha E I, Shashkov E V, Kelly T, et al. *In vivo* magnetic enrichment and multiplex photoacoustic detection of circulating tumour cells[J]. Nature Nanotechnology, 2009, 4: 855-860.

[48] Wang H W, Chai N, Wang P, et al. Label-free bond-selective imaging by listening to vibrationally excited molecules[J]. Physical Review Letters, 2011, 106(23): 238106.

[49] Visscher M, Pleitez M A, van Gaalen K, et al. Label-free analytic histology of carotid atherosclerosis by mid-infrared optoacoustic microscopy[J]. Photoacoustics, 2022, 26: 100354.

[50] Jin Y Y, Yin Y G, Li C Y, et al. Non-invasive monitoring of human health by photoacoustic spectroscopy [J]. Sensors, 2022, 22(3): 1155.

[51] Kaysir M R, Song J Q, Rassel S, et al. Progress and perspectives of mid-infrared photoacoustic spectroscopy for non-invasive glucose detection[J]. Biosensors, 2023, 13(7): 716.

[52] Wang X D, Ku G, Wegiel M A, et al. Noninvasive photoacoustic angiography of animal brains in vivo with near-infrared light and an optical contrast agent[J]. Optics Letters, 2004, 29(7): 730-732.

[53] Hugon O, van der Sanden B, Inglebert M, et al. Multi-wavelength photo-acoustic microscopy in the frequency domain for simultaneous excitation and detection of dyes [J]. Biomedical Optics Express, 2019, 10(2): 932-943.

[54] Aoki H, Nojiri M, Mukai R, et al. Near-infrared absorbing polymer nano-particle as a sensitive contrast agent for photo-acoustic imaging[J]. Nanoscale, 2015, 7(1): 337-343.

[55] Nguyen V P, Li Y X, Henry J, et al. Gold nanorod

enhanced photoacoustic microscopy and optical coherence tomography of choroidal neovascularization[J]. ACS Applied Materials & Interfaces, 2021, 13(34): 40214-40228.

[56] Razansky D, Distel M, Vinegoni C, et al. Multispectral opto-acoustic tomography of deep-seated fluorescent proteins *in vivo*[J]. Nature Photonics, 2009, 3: 412-417.

[57] Ning B, Sun N D, Cao R, et al. Ultrasound-aided multi-parametric photoacoustic microscopy of the mouse brain [J]. Scientific Reports, 2015, 5: 18775.

[58] Strohm E M, Berndl E S L, Kolios M C. High frequency label-free photoacoustic microscopy of single cells[J]. Photoacoustics, 2013, 1(3): 49-53.

[59] Wang L D, Zhang C, Wang L V. Grueneisen relaxation photoacoustic microscopy[J]. Physical Review Letters, 2014, 113(17): 174301.

[60] Yao J J, Wang L D, Yang J M, et al. High-speed label-free functional photoacoustic microscopy of mouse brain in action[J]. Nature Methods, 2015, 12: 407-410.

[61] Yao D K, Maslov K, Shung K K, et al. *In vivo* label-free photoacoustic microscopy of cell nuclei by excitation of DNA and RNA[J]. Optics Letters, 2010, 35(24): 4139-4141.

[62] Ye S Q, Yang R, Xiong J W, et al. Label-free imaging of zebrafish larvae *in vivo* by photoacoustic microscopy [J]. Biomedical Optics Express, 2012, 3(2): 360-365.

[63] Chen Q, Jin T, Qi W Z, et al. Label-free photoacoustic imaging of the cardio-cerebrovascular development in the embryonic zebrafish[J]. Biomedical Optics Express, 2017, 8(4): 2359-2367.

[64] Maslov K, Zhang H F, Wang L V. Portable real-time photoacoustic microscopy[J]. Proceedings of SPIE, 2007, 6437: 643727.

[65] Zhou Y, Xing W X, Maslov K I, et al. Handheld photoacoustic microscopy to detect melanoma depth *in vivo*[J]. Optics Letters, 2014, 39(16): 4731-4734.

[66] Zeng L M, Liu G D, Yang D W, et al. Portable optical-resolution photoacoustic microscopy with a pulsed laser diode excitation[J]. Applied Physics Letters, 2013, 102 (5): 053704.

[67] Wang L D, Maslov K, Yao J J, et al. Fast voice-coil scanning optical-resolution photoacoustic microscopy[J]. Optics Letters, 2011, 36(2): 139-141.

[68] Wang L D, Maslov K, Xing W X, et al. Video-rate functional photoacoustic microscopy at depths[J]. Journal of Biomedical Optics, 2012, 17(10): 106007.

[69] Wang L D, Maslov K, Wang L V. Single-cell label-free photoacoustic flowoxigraphy *in vivo*[J]. Proceedings of the National Academy of Sciences of the United States of America, 2013, 110(15): 5759-5764.

[70] Hajireza P, Shi W, Zemp R J. Real-time handheld optical-resolution photoacoustic microscopy[J]. Optics Express, 2011, 19(21): 20097-20102.

[71] Zhang W Y, Ma H G, Cheng Z W, et al. Miniaturized photoacoustic probe for *in vivo* imaging of subcutaneous microvessels within human skin[J]. Quantitative Imaging in Medicine and Surgery, 2019, 9(5): 807-814.

[72] Seong D, Han S, Lee J, et al. Waterproof galvanometer scanner-based handheld photoacoustic microscopy probe for wide-field vasculature imaging in vivo[J]. Photonics for Solar Energy Systems IX, 2021, 8(8): 305.

[73] Jin T, Guo H, Jiang H B, et al. Portable optical resolution photoacoustic microscopy (pORPAM) for human oral imaging[J]. Optics Letters, 2017, 42(21): 4434-4437.

[74] Jin T, Guo H, Yao L, et al. Portable optical-resolution photoacoustic microscopy for volumetric imaging of multiscale organisms[J]. Journal of Biophotonics, 2018, 11(4): e201700250.

[75] Jin T, Qi W Z, Liang X, et al. Photoacoustic imaging of brain functions: wide filed-of-view functional imaging with high spatiotemporal resolution[J]. Laser & Photonics Reviews, 2022, 16(2): 2100304.

[76] Qin W, Gan Q, Yang L, et al. High-resolution *in vivo* imaging of rhesus cerebral cortex with ultrafast portable photoacoustic microscopy[J]. NeuroImage, 2021, 238: 118260.

[77] Chen J B, Zhang Y C, Zhu J Y, et al. Freehand scanning photoacoustic microscopy with simultaneous localization and mapping[J]. Photoacoustics, 2022, 28: 100411.

[78] Lin L, Zhang P F, Xu S, et al. Handheld optical-resolution photoacoustic microscopy[J]. Journal of Biomedical Optics, 2017, 22(4): 041002.

[79] Park K, Kim J Y, Lee C, et al. Handheld photoacoustic microscopy probe[J]. Scientific Reports, 2017, 7: 13359.

[80] Qi W Z, Chen Q, Guo H, et al. Miniaturized optical resolution photoacoustic microscope based on a microelectro mechanical systems scanning mirror[J]. Micromachines, 2018, 9(6): 288.

[81] Guo H, Chen Q, Qi W Z, et al. *In vivo* study of rat cortical hemodynamics using a stereotaxic-apparatus-compatible photoacoustic microscope[J]. Journal of Biophotonics, 2018, 11(9): e201800067.

[82] Zhang W Y, Ma H G, Cheng Z W, et al. High-speed dual-view photoacoustic imaging pen[J]. Optics Letters, 2020, 45(7): 1599-1602.

[83] Kim J, Kim J Y, Jeon S, et al. Super-resolution localization photoacoustic microscopy using intrinsic red blood cells as contrast absorbers[J]. Light: Science & Applications, 2019, 8: 103.

[84] Kim J Y, Lee C, Park K, et al. High-speed and high-SNR photoacoustic microscopy based on a galvanometer mirror in non-conducting liquid[J]. Scientific Reports, 2016, 6: 34803.

[85] Qin W, Jin T, Guo H, et al. Large-field-of-view optical resolution photoacoustic microscopy[J]. Optics Express, 2018, 26(4): 4271-4278.

[86] Lee J, Han S, Seong D, et al. Fully waterproof two-axis galvanometer scanner for enhanced wide-field optical-resolution photoacoustic microscopy[J]. Optics Letters, 2020, 45(4): 865-868.

[87] Zhong F H, Hu S. Thin-film optical-acoustic combiner enables high-speed wide-field multi-parametric photoacoustic microscopy in reflection mode[J]. Optics Letters, 2023,

48(2): 195-198.

[88] Qi W Z, Liang X, Ji Y Y, et al. Optical resolution photoacoustic computed microscopy[J]. Optics Letters, 2021, 46(2): 372-375.

[89] Li L Y, Qin W, Li T T, et al. High-speed adaptive photoacoustic microscopy[J]. Photonics Research, 2023, 11(12): 2084-2092.

[90] Yao J J, Wang L D, Yang J M, et al. Wide-field fast-scanning photoacoustic microscopy based on a water-immersible MEMS scanning mirror[J]. Journal of Biomedical Optics, 2012, 17(8): 080505.

[91] Kim J Y, Lee C, Park K, et al. Fast optical-resolution photoacoustic microscopy using a 2-axis water-proofing MEMS scanner[J]. Scientific Reports, 2015, 5: 7932.

[92] Zhang C, Zhao H X, Xu S, et al. Multiscale high-speed photoacoustic microscopy based on free-space light transmission and a MEMS scanning mirror[J]. Optics Letters, 2020, 45(15): 4312-4315.

[93] Lee C, Kim J Y, Kim C. Recent progress on photoacoustic imaging enhanced with microelectromechanical systems (MEMS) technologies[J]. Micromachines, 2018, 9(11): 584.

[94] Ahn J, Kim J Y, Choi W, et al. High-resolution functional photoacoustic monitoring of vascular dynamics in human fingers[J]. Photoacoustics, 2021, 23: 100282.

[95] Wang Y, Zhang R, Chen Q, et al. Visualization of blood-brain barrier disruption with dual-wavelength high-resolution photoacoustic microscopy[J]. Biomedical Optics Express, 2022, 13(3): 1537-1550.

[96] Yao J J, Xia J, Maslov K I, et al. Noninvasive photoacoustic computed tomography of mouse brain metabolism *in vivo*[J]. NeuroImage, 2013, 64: 257-266.

[97] Na S, Wang L V. Photoacoustic computed tomography for functional human brain imaging[J]. Biomedical Optics Express, 2021, 12(7): 4056-4083.

[98] Yang X, Chen Y H, Xia F, et al. Photoacoustic imaging for monitoring of stroke diseases: a review[J]. Photoacoustics, 2021, 23: 100287.

[99] Yao J J, Kaberniuk A A, Li L, et al. Multiscale photoacoustic tomography using reversibly switchable bacterial phytochrome as a near-infrared photochromic probe[J]. Nature Methods, 2016, 13: 67-73.

[100] Meimani N, Abani N, Gelovani J, et al. A numerical analysis of a semi-dry coupling configuration in photoacoustic computed tomography for infant brain imaging[J]. Photoacoustics, 2017, 7: 27-35.

[101] Tang J B, Coleman J E, Dai X J, et al. Wearable 3-D photoacoustic tomography for functional brain imaging in behaving rats[J]. Scientific Reports, 2016, 6: 25470.

[102] Na S, Russin J J, Lin L, et al. Massively parallel functional photoacoustic computed tomography of the human brain[J]. Nature Biomedical Engineering, 2022, 6: 584-592.

[103] Cao R, Li J, Ning B, et al. Functional and oxygen-metabolic photoacoustic microscopy of the awake mouse brain[J]. NeuroImage, 2017, 150: 77-87.

[104] Cao R, Li J, Zhang C C, et al. Photoacoustic microscopy of obesity-induced cerebrovascular alterations [J]. NeuroImage, 2019, 188: 369-379.

[105] Govinahallisathyanarayana S, Ning B, Cao R, et al. Dictionary learning-based reverberation removal enables depth-resolved photoacoustic microscopy of cortical microvasculature in the mouse brain[J]. Scientific Reports, 2018, 8: 985.

[106] Sciortino V M, Tran A, Sun N D, et al. Longitudinal cortex-wide monitoring of cerebral hemodynamics and oxygen metabolism in awake mice using multi-parametric photoacoustic microscopy[J]. Journal of Cerebral Blood Flow and Metabolism, 2021, 41(12): 3187-3199.

[107] Xi L, Jin T, Zhou J L, et al. Hybrid photoacoustic and electrophysiological recording of neurovascular communications in freely-moving rats[J]. NeuroImage, 2017, 161: 232-240.

[108] Chen Q, Xie H K, Xi L. Wearable optical resolution photoacoustic microscopy[J]. Journal of Biophotonics, 2019, 12(8): e201900066.

[109] Dangi A, Agrawal S, Datta G R, et al. Towards a low-cost and portable photoacoustic microscope for point-of-care and wearable applications[J]. IEEE Sensors Journal, 2020, 20(13): 6881-6888.

[110] Guo H, Chen Q, Qin W, et al. Detachable head-mounted photoacoustic microscope in freely moving mice [J]. Optics Letters, 2021, 46(24): 6055-6058.

[111] Nguyen V P, Fan W, Zhu T Y, et al. Multimodal photoacoustic microscopy, optical coherence tomography, and fluorescence *in vivo* tracking of stem cells[C]//2022 Conference on Lasers and Electro-Optics (CLEO), May 15-20, 2022, San Jose, CA, USA. New York: IEEE Press, 2022.

[112] Song W, Wei Q, Liu W Z, et al. A combined method to quantify the retinal metabolic rate of oxygen using photoacoustic ophthalmoscopy and optical coherence tomography[J]. Scientific Reports, 2014, 4: 6525.

[113] Zhang W, Li Y X, Nguyen V P, et al. High-resolution, *in vivo* multimodal photoacoustic microscopy, optical coherence tomography, and fluorescence microscopy imaging of rabbit retinal neovascularization[J]. Light: Science & Applications, 2018, 7: 103.

[114] Li Y X, Zhang W, Nguyen V P, et al. Real-time OCT guidance and multimodal imaging monitoring of subretinal injection induced choroidal neovascularization in rabbit eyes[J]. Experimental Eye Research, 2019, 186: 107714.

[115] Li L, Rao B, Maslov K, et al. Fast-scanning reflection-mode integrated photoacoustic and optical-coherence microscopy[J]. Proceedings of SPIE, 2010, 7564: 75641Z.

[116] Liu M Y, Chen Z, Zabihian B, et al. Combined multi-modal photoacoustic tomography, optical coherence tomography (OCT) and OCT angiography system with an articulated probe for in vivo human skin structure and vasculature imaging[J]. Biomedical Optics Express, 2016, 7(9): 3390-3402.

[117] Dadkhah A, Jiao S L. Integrating photoacoustic

microscopy with other imaging technologies for multimodal imaging[J]. Experimental Biology and Medicine, 2021, 246(7): 771-777.

[118] Kukk A F, Wu D, Gaffal E, et al. Multimodal imaging system with ultrasound, photoacoustics, and optical coherence tomography for optical biopsy of melanoma[J]. Proceedings of SPIE, 2023, 12371: 1237107.

[119] Dadkhah A, Jiao S. Integrating photoacoustic microscopy, optical coherence tomography, OCT angiography, and fluorescence microscopy for multimodal imaging[J]. Experimental Biology and Medicine, 2020, 245(4): 342-347.

[120] Liu C B, Liao J L, Chen L C, et al. The integrated high-resolution reflection-mode photoacoustic and fluorescence confocal microscopy[J]. Photoacoustics, 2019, 14: 12-18.

[121] Zhou J S, Wang W, Jing L L, et al. Dual-modal imaging with non-contact photoacoustic microscopy and fluorescence microscopy[J]. Optics Letters, 2021, 46(5): 997-1000.

[122] Zhang W, Li Y X, Yu Y X, et al. Simultaneous photoacoustic microscopy, spectral-domain optical coherence tomography, and fluorescein microscopy multi-modality retinal imaging[J]. Photoacoustics, 2020, 20: 100194.

[123] Chen S L, Xie Z X, Guo L J, et al. A fiber-optic system for dual-modality photoacoustic microscopy and confocal fluorescence microscopy using miniature components[J]. Photoacoustics, 2013, 1(2): 30-35.

[124] Huang D, Swanson E A, Lin C P, et al. Optical coherence tomography[J]. Science, 1991, 254(5035): 1178-1181.

[125] de Boer J F, Leitgeb R, Wojtkowski M. Twenty-five years of optical coherence tomography: the paradigm shift in sensitivity and speed provided by Fourier domain OCT [J]. Biomedical Optics Express, 2017, 8(7): 3248-3280.

[126] Psomadakis C E, Marghoob N, Bleicher B, et al. Optical coherence tomography[J]. Clinics in Dermatology, 2021, 39(4): 624-634.

[127] Li L, Maslov K, Ku G, et al. Three-dimensional combined photoacoustic and optical coherence microscopy for *in vivo* microcirculation studies[J]. Optics Express, 2009, 17(19): 16450-16455.

[128] Jiao S L, Xie Z X, Zhang H F, et al. Simultaneous multimodal imaging with integrated photoacoustic microscopy and optical coherence tomography[J]. Optics Letters, 2009, 34(19): 2961-2963.

[129] Liu T, Wei Q, Wang J, et al. Combined photoacoustic microscopy and optical coherence tomography can measure metabolic rate of oxygen[J]. Biomedical Optics Express, 2011, 2(5): 1359-1365.

[130] Zhu X Y, Huang Z Y, Li Z Y, et al. Resolution-matched reflection mode photoacoustic microscopy and optical coherence tomography dual modality system[J]. Photoacoustics, 2020, 19: 100188.

[131] Haindl R, Deloria A J, Sturtzel C, et al. Functional optical coherence tomography and photoacoustic microscopy imaging for zebrafish larvae[J]. Biomedical Optics Express, 2020, 11(4): 2137-2151.

[132] Xi L, Duan C, Xie H K, et al. Miniature probe combining optical-resolution photoacoustic microscopy and optical coherence tomography for *in vivo* microcirculation study[J]. Applied Optics, 2013, 52(9): 1928-1931.

[133] Qin W, Qi W Z, Jin T, et al. *In vivo* oral imaging with integrated portable photoacoustic microscopy and optical coherence tomography[J]. Applied Physics Letters, 2017, 111(26): 263704.

[134] Qin W, Chen Q, Xi L. A handheld microscope integrating photoacoustic microscopy and optical coherence tomography[J]. Biomedical Optics Express, 2018, 9(5): 2205-2213.

[135] Bai X S, Gong X J, Hau W, et al. Intravascular optical-resolution photoacoustic tomography with a 1.1 mm diameter catheter[J]. PLoS One, 2014, 9(3): e92463.

[136] Gerling M, Zhao Y, Nania S, et al. Real-time assessment of tissue hypoxia *in vivo* with combined photoacoustics and high-frequency ultrasound[J]. Theranostics, 2014, 4(6): 604-613.

[137] Subochev P, Orlova A, Shirmanova M, et al. Simultaneous photoacoustic and optically mediated ultrasound microscopy: an *in vivo* study[J]. Biomedical Optics Express, 2015, 6(2): 631-638.

[138] Daoudi K, Kersten B E, van den Ende C H M, et al. Photoacoustic and high-frequency ultrasound imaging of systemic sclerosis patients[J]. Arthritis Research & Therapy, 2021, 23(1): 22.

[139] Daoudi K, van den Berg P J, Rabot O, et al. Handheld probe integrating laser diode and ultrasound transducer array for ultrasound/photoacoustic dual modality imaging [J]. Optics Express, 2014, 22(21): 26365-26374.

[140] Yang Y, Li X, Wang T H, et al. Integrated optical coherence tomography, ultrasound and photoacoustic imaging for ovarian tissue characterization[J]. Biomedical Optics Express, 2011, 2(9): 2551-2561.

[141] Li Y, Lu G X, Zhou Q F, et al. Advances in endoscopic photoacoustic imaging[J]. Photonics, 2021, 8(7): 281.

[142] Park J, Park B, Kim T Y, et al. Quadruple ultrasound, photoacoustic, optical coherence, and fluorescence fusion imaging with a transparent ultrasound transducer[J]. Proceedings of the National Academy of Sciences of the United States of America, 2021, 118(11): e1920879118.

[143] 万余洋, 雷鹏, 熊科迪, 等. 血管内光声-超声-光学相干层析-光声弹性多模态成像方法及系统[J]. 中国激光, 2023, 50(3): 0307107.
Wan Y Y, Lei P, Xiong K D, et al. Intravascular photoacoustic, ultrasonic, optical coherence tomography, and photoacoustic elastic multimodal imaging method and system[J]. Chinese Journal of Lasers, 2023, 50(3): 0307107.

[144] Dai X J, Xi L, Duan C, et al. Miniature probe integrating optical-resolution photoacoustic microscopy, optical coherence tomography, and ultrasound imaging: proof-of-concept[J]. Optics Letters, 2015, 40(12): 2921-2924.

[145] Dai X J, Yang H, Shan T Q, et al. Miniature endoscope for multimodal imaging[J]. ACS Photonics, 2017, 4(1):

174-180.

[146] Leng J, Zhang J K, Li C G, et al. Multi-spectral intravascular photoacoustic/ultrasound/optical coherence tomography tri-modality system with a fully-integrated 0.9-mm full field-of-view catheter for plaque vulnerability imaging[J]. Biomedical Optics Express, 2021, 12(4): 1934-1946.

[147] Huang B X, Wong T T W. Review of low-cost light sources and miniaturized designs in photoacoustic microscopy[J]. Journal of Biomedical Optics, 2024, 29 (Suppl 1): S11503.

[148] Chen S L, Xie Z X, Ling T, et al. Miniaturized all-optical photoacoustic microscopy based on microelectromechanical systems mirror scanning[J]. Optics Letters, 2012, 37(20): 4263-4265.

[149] Guo Z D, Li G Y, Chen S L. Miniature probe for all-optical double gradient-index lenses photoacoustic microscopy[J]. Journal of Biophotonics, 2018, 11(12): e201800147.

[150] Guo Z D, Li Y, Chen S L. Miniature probe for *in vivo* optical- and acoustic-resolution photoacoustic microscopy [J]. Optics Letters, 2018, 43(5): 1119-1122.

[151] Chen Q, Qin W, Qi W Z, et al. Progress of clinical translation of handheld and semi-handheld photoacoustic imaging[J]. Photoacoustics, 2021, 22: 100264.

[152] Wang K Y, Li C Y, Chen R M, et al. Recent advances in high-speed photoacoustic microscopy[J]. Photoacoustics, 2021, 24: 100294.

[153] Chen X X, Qi W Z, Xi L. Deep-learning-based motion-correction algorithm in optical resolution photoacoustic microscopy[J]. Visual Computing for Industry, Biomedicine, and Art, 2019, 2(1): 12.

[154] Zhao H X, Ke Z W, Yang F, et al. Deep learning enables superior photoacoustic imaging at ultralow laser dosages[J]. Advanced Science, 2020, 8(3): 2003097.

[155] Gao Y, Xu W Y, Chen Y M, et al. Deep learning-based photoacoustic imaging of vascular network through thick porous media[J]. IEEE Transactions on Medical Imaging, 2022, 41(8): 2191-2204.

[156] Gröhl J, Schellenberg M, Dreher K, et al. Deep learning for biomedical photoacoustic imaging: a review[J]. Photoacoustics, 2021, 22: 100241.

[157] Yang C C, Lan H R, Gao F, et al. Review of deep learning for photoacoustic imaging[J]. Photoacoustics, 2021, 21: 100215.

[158] Tserevelakis G J, Barmparis G D, Kokosalis N, et al. Deep learning-assisted frequency-domain photoacoustic microscopy[J]. Optics Letters, 2023, 48(10): 2720-2723.

[159] Hosseinaee Z, Le M, Bell K, et al. Towards non-contact photoacoustic imaging[J]. Photoacoustics, 2020, 20: 100207.

[160] Wissmeyer G, Pleitez M A, Rosenthal A, et al. Looking at sound: optoacoustics with all-optical ultrasound detection[J]. Light: Science & Applications, 2018, 7: 53.

[161] Wang Y, Hu Y X, Peng B Y, et al. Complete-noncontact photoacoustic microscopy by detection of initial pressures using a 3 × 3 coupler-based fiber-optic interferometer[J]. Biomedical Optics Express, 2019, 11 (1): 505-516.

[162] Hosseinaee Z, Khalili L, Simmons J A T, et al. Label-free, non-contact, *in vivo* ophthalmic imaging using photoacoustic remote sensing microscopy[J]. Optics Letters, 2020, 45(22): 6254-6257.

[163] Manwar R, Kratkiewicz K, Avanaki K. Overview of ultrasound detection technologies for photoacoustic imaging[J]. Micromachines, 2020, 11(7): 692.

[164] Park S, Rim S, Kim Y, et al. Noncontact photoacoustic imaging based on optical quadrature detection with a multiport interferometer[J]. Optics Letters, 2019, 44 (10): 2590-2593.